MODELING OF DROPWISE CONDENSATION ON FLAT SURFACES

Riccardo Parin, Andrea Penazzato, Stefano Bortolin, Davide Del Col*

*Author for correspondence
Department of Industrial Engineering
University of Padova, Via Venezia, 1
35131 - Padova, Italy
E-mail: davide.delcol@unipd.it

ABSTRACT

There are two ways for a vapor to condense on a surface: filmwise condensation (FWC) and dropwise condensation (DWC). The interest in DWC is based on the potential increase of the condensation heat transfer coefficient (HTC) by 6 to 10 times compared to the values measured during filmwise condensation. For this reason, several research groups around the world have tried to promote the dropwise condensation and to describe the underneath mechanisms. Such models describe the phenomena that take place during dropwise condensation: the nucleation of a droplet until its departure, the heat exchanged by the drop during its lifetime and the droplets population on the surface.

The present paper aims at presenting some of the models developed in the past years which can be used to describe the DWC process. In particular, similarities and differences between the models are highlighted and their predictions are compared against experimental data measured at the Two-phase Heat Transfer Laboratory of the University of Padova.

INTRODUCTION

In 1930, for the first time, dropwise condensation was described in a scientific paper [1] and the heat transfer potential of this type of condensation, as compared to the filmwise condensation mode, was highlighted. Dropwise condensation is usually obtained when the surface is hydrophobic: the surface induces the breakage of the liquid film that normally fully wets the surface, replacing it with a large amount of randomly distributed droplets. The study of the DWC aroused a discontinuous interest from the heat transfer community, and the first semi-empirical models were developed only starting from the second half of the 60s [2]. After this period, to find other publications about this topic, we have to wait until the end of 90s and particularly until the beginning of new millennium [3–5]. Indeed, in recent years, the material science has made major progress in the development of new surfaces that could favor dropwise condensation. Moreover, researchers have focused their attention on micro- and nanostructured surfaces displaying superhydrophobic characteristics [6] which may lead to even higher heat transfer coefficients promoting the phenomenon of "jumping droplets".

The present work deals with dropwise condensation on flat surfaces and thus without considering the presence of artificial roughness that, for example, is necessary to realize the aforementioned superhydrophobic substrates. Several heat transfer models that can be used during DWC on flat surfaces have been proposed in the literature and, in the present paper, three different studies have been selected: Le Fevre and Rose as reported in Rose [2], Abu-Orabi [3], and the recent work by Kim *et al.* [4]. The results calculated by the models are compared with some experimental data taken on hydrophobic polished aluminum substrates by the present research group. Heat transfer coefficients have been measured in a two-phase thermosiphon loop during pure steam dropwise condensation over plain vertical surfaces. A high-speed camera has been used to study the different parameters affecting the DWC phenomenon, such as the droplet departing radius and the population of "large" droplets.

NOMENCLATURE

A	[m^2]	area
g	[$m\ s^{-2}$]	gravity acceleration
G	[$m\ s^{-1}$]	drop growth rate
h	[$J\ kg^{-1}$]	specific enthalpy
h_i	[$W\ m^{-2}\ K^{-1}$]	interfacial heat transfer coefficient
HTC	[$kW\ m^{-2}\ K^{-1}$]	heat transfer coefficient
$\dot{m}$	[$kg\ s^{-1}$]	mass flow rate
n	[m^{-3}]	"small" drop population
N	[m^{-3}]	"large" drop population
N_s	[m^{-2}]	nucleation sites
q	[kW]	heat flow rate
q'	[$kW\ m^{-2}$]	heat flux
r	[m]	radius
R	[$J\ mol^{-1}\ K^{-1}$]	gas constant
S	[$m^2\ s^{-1}$]	surface renewal
t	[°C]	temperature
T	[K]	temperature
v	[$m\ s^{-1}$]	velocity
Greeks		
α	[-]	accommodation coefficient
γ	[-]	ratio of the specific heat capacities
δ	[m]	thickness
θ	[°]	contact angle
λ	[$W\ m^{-1}\ K^{-1}$]	thermal conductivity
ρ	[$kg\ m^{-3}$]	density
σ	[$N\ m^{-1}$]	surface tension
τ	[s]	sweeping period

Subscripts

a	advancing
c	curvature
d	drop
e	effective
coat	coating
cool	coolant
l	liquid
max	maximum
min	minimum
r	receding
SAT	saturation
v	vapor
WALL	wall

THEORETICAL MODELS

The dropwise condensation starts at molecular level, with the formation of small clusters of molecules (minimum radius r_{min}) in a number of preferential nucleation sites (N_s), which grow by direct condensation of steam on them. Subsequently, due to the proximity of the nucleation sites, the drops come into contact with each other, they coalescence (effective radius r_e) and, when maximum radius r_{max} is reached (the external forces exceed the adhesion force which allows them to remain attached to the surface), the drops begin to slip away. While slipping, the droplets continue to grow for coalescing with other droplets that they encounter along their path leaving the surface clean and available for the formation of new nuclei [7]. All the three models considered in the present paper account for the aforementioned mechanisms.

Since during DWC the whole surface is covered by a large amount of droplets randomly distributed with different sizes, a distribution function of the droplet population has to be defined. Therefore, knowing the heat exchanged by a single drop and the number of droplets per unit area, the heat flux can be calculated through the operation of integration from the minimum radius to the maximum one. So, naming $n(r)$ the "small" droplets population ($r < r_e$) and $N(r)$ the population of "large" droplets ($r > r_e$), it follows that:

$$q' = \int_{r_{min}}^{r_e} q_d(r) \cdot n(r) dr + \int_{r_e}^{r_{max}} q_d(r) \cdot N(r) dr \quad (1)$$

The heat transfer coefficient is calculated as:

$$\mathrm{HTC} = q'/\Delta T \quad (2)$$

where ΔT is the temperature difference between the saturation temperature (t_{SAT}) and the surface temperature (t_{WALL}). The minimum droplet radius is defined when a cluster of molecules is in equilibrium with the surface and it is calculated as [7]

$$r_{min} = \frac{2\sigma v_l}{h_{lv}(t_{SAT} - t_{WALL})} \quad (3)$$

where σ is the surface tension, v_l is the specific volume of the saturated liquid and h_{lv} the specific enthalpy of evaporation.

Le Fevre and Rose model (1966)

The first model developed for dropwise condensation was proposed by Le Fevre and Rose [2] in 1966. The heat flow rate through a single drop is obtained with a semi-empirical relationship:

$$q_d(r) = \frac{\Delta T - \frac{2\sigma T_{SAT}}{r\,\rho_l h_{lv}}}{K_1 \frac{r}{\lambda_l} + K_2 \left(\frac{0.627}{0.664}\right) \frac{T_{SAT}}{h_{lv}^2 \rho_l} \frac{\gamma+1}{\gamma-1} \left[\frac{RT_{SAT}}{2\pi}\right]^{0.5}} \quad (4)$$

where K_1 and K_2 are constants imposed by the authors, λ_l is the liquid conductivity, ρ_l is the liquid density, γ is the ratio of the specific heat capacities and R is the ideal-gas constant. At the numerator, in addition to the temperature difference ΔT, the effect of the droplet curvature is taken into account. At the denominator, the first term represents the resistance to the heat conduction through the condensate, meanwhile, the second term represents the resistance to the mass transport at the interface between vapor and liquid. The droplet population covers only the "large" droplets with the expression:

$$N(r) = \frac{1}{3\pi r^2 r_{max}} \left(\frac{r}{r_{max}}\right)^{-\frac{2}{3}} \quad (5)$$

where the maximum radius is defined as:

$$r_{max} = K_3 \left[\frac{\sigma}{\rho g}\right]^{\frac{1}{2}} \quad (6)$$

K_3 is a constant and g is the gravity acceleration. Hereafter, Eq. (5) will be used for all the three models. As a final step, the heat flux is determined by Eq. (1).

Abu-Orabi model (1998)

The model developed in 1998 by Abu-Orabi [3] was the first that computes the heat transfer through a single drop by incorporating the various thermal resistances from the vapor to the surface and considers both the populations of "small" and "large" droplets as proposed in [8,9]. The thermal resistances can be evaluated as the ratio between temperature drop and heat flow rate q_d; in particular the temperature drop due to the interfacial resistance is:

$$\Delta T_i = \frac{q_d}{h_i 2\pi r^2} \quad (7)$$

where h_i is the interfacial heat transfer coefficient, which includes the accommodation coefficient (α). The experimental data used in this paper are taken in saturated conditions of steam, thus α is assumed equal to 1 as suggested in [3]. The thermal resistance due to heat conduction through the drop can be estimated from Eq. (8)

$$\Delta T_d = \frac{q_d r}{4\pi r^2 \lambda_l} \quad (8)$$

The promoting layer on the substrate adds a temperature drop equal to:

$$\Delta T_{coat} = \frac{q_d \delta}{4\pi r^2 \lambda_{coat}} \quad (9)$$

where δ is the layer thickness. Finally, the droplet curvature gives a temperature variation

$$\Delta T_c = \frac{2T_{SAT}\sigma}{h_{lv} r \rho_l} \quad (10)$$

From Eqs. (7-10) and considering Eq. (3), the heat flow rate through a single drop of radius r can be calculated as:

$$q_d(r) = \frac{4\pi r^2\left(1-\frac{r_{min}}{r}\right)\Delta T}{\left(\frac{\delta}{\lambda_{coat}}+\frac{r}{\lambda_l}+\frac{2}{h_i}\right)} \quad (11)$$

With regard to the droplet population, the author extends the Le Fevre and Rose analysis (Eq. (5)) in order to add the "small" droplet population. For the sake of brevity, only the main Eqs. are reported in the following. Assuming that in a given surface area A, the number of entering droplets is equal to the number of leaving droplets plus the droplets swept and assuming the growth rate for a drop [9] equal to

$$G = \frac{dr}{dt} \quad (12)$$

the droplet balance in that area will be:

$$An_1G_1\Delta t = An_2G_2\Delta t + S\bar{n}\Delta r\Delta t \quad (13)$$

where n is the number of drops per unit area per unit drop radius, S is the rate at which the substrate surface is renewed due to sweeping, $\bar{n}$ is the average population density in the size range r_1 to r_2, $\Delta r = r_2$-r_1, and Δt is an increment of time. For $\Delta r \to 0$, the Eq. (13) becomes

$$G\frac{dn}{dr} + n\frac{dG}{dr} + \frac{n}{\tau} = 0 \quad (14)$$

where $\tau = A/S$ is the sweeping period. As a boundary condition, the authors impose that the population of "small" droplets equals that of "large" droplets at r_e:

$$n(r_e) = N(r_e) \quad (15)$$

where r_e is calculated assuming that the nucleation sites form a square array, $r_e = 1/\sqrt{4N_s}$; the Eq. (14) can be integrated with respect to r, obtaining:

$$n(r) = N(r_e)\frac{r(r_e-r_{min})(A_2r+A_3)}{r_e(r-r_{min})(A_2r_e+A_3)}e^{B_1+B_2} \quad (16)$$

where

$$B_1 = \frac{A_2}{A_1\tau}\left[\frac{{r_e}^2-r^2}{2} + r_{min}(r_e-r_{min}) - {r_{min}}^2\ln\left(\frac{r-r_{min}}{r_e-r_{min}}\right)\right] \quad (17)$$

$$B_2 = \frac{A_3}{A_1\tau}\left[(r_e-r) - r_{min}\ln\left(\frac{r-r_{min}}{r_e-r_{min}}\right)\right] \quad (18)$$

$$\tau = \frac{3{r_e}^2(A_2r+A_3)^2}{A_1[8A_3r_e-14A_2r_er_{min}+11A_2{r_e}^2-11A_3r_{min}]} \quad (19)$$

The three parameters (A_1, A_2, and A_3) in Eqs. (16-19) are defined as:

$$A_1 = \frac{2\Delta T}{\rho_l h_{lv}};\quad A_2 = \frac{1}{\lambda_l};\quad A_3 = \frac{2}{h_i} + \frac{\delta}{\lambda_{coat}} \quad (20)$$

which are derived from Eq. (11) by means of Eq. (12) and Eq. (21) (heat exchanged through a drop)

$$q_d(r) = \rho_l h_{lv}\left(2\pi r\frac{dr}{dt}\right) \quad (21)$$

Kim *et al.* model (2011)

Both the previous models assume that the droplets grow during dropwise condensation with a hemispherical shape, i.e. a contact angle (θ) between solid and liquid equal to 90°. However, liquids wet the surface with different contact angles depending on the surface tension balance at the triple line [6]. The model of Kim *et al.* [4] introduces the contact angle as a variable in order to fill this gap. The authors studied how the contact angle influences the dropwise condensation performances in the range from 90° to 150°. Since the roughness is not considered, using water as a working fluid, the analysis should stop at about 120°. A similar approach to the one proposed by Abu-Orabi is considered: the thermal resistances from the vapor to the surface are considered and, in this case, the droplet growing angle is also accounted for. In particular, the resistance due to conduction in the drop can be obtained from:

$$\Delta T_d = \frac{q_d\theta}{4\pi r\lambda_l\sin\theta} \quad (22)$$

Eq. (22) changes dramatically the conduction through a single droplet, giving to the droplets their natural spherical shape instead of a flat layer as in Le Fevre and Rose and Abu-Orabi. The heat flow through the single drop is calculated as:

$$q_d(r) = \frac{\Delta T\pi r^2\left(1-\frac{r_{min}}{r}\right)}{\left(\frac{\delta}{\lambda_{coat}\sin\theta^2}+\frac{r\theta}{4\lambda_l\sin\theta}+\frac{1}{2h_i(1-\cos\theta)}\right)} \quad (23)$$

Also this model considers a division between "large" and "small" droplets. The coefficients for "small" droplets population (Eq. 16) are:

$$A_1 = \frac{2\Delta T}{\rho_l h_{lv}};\ A_2 = \frac{\vartheta(1-\cos(\vartheta))}{4\,\lambda_l\sin(\vartheta)};\ A_3 = \frac{1}{2\,h_i} + \frac{\delta(1-\cos(\vartheta))}{\lambda_{coat}\sin(\vartheta)^2} \quad (24)$$

In the model, the maximum droplet radius reached during dropwise condensation on a vertical surface is obtained from the balance between the capillary force and the gravity force:

$$r_{max} = \sqrt{\frac{6(\cos(\vartheta_r)-\cos(\vartheta_a))\sin(\vartheta)}{\pi(2-3\cos(\vartheta)+cos^2(\vartheta))}\frac{\sigma}{\rho_l g}} \quad (25)$$

where θ_a and θ_r are the advancing and receding contact angles, respectively.

THEORETICAL MODELS COMPARISON

The first model proposed by Le Fevre and Rose needs the properties of the fluid (calculated at the saturation temperature T_{sat}) and the wall temperature as input values. Instead, in the model by Abu-Orabi, due to its increased complexity, in addition to the properties of the hydrophobic layer (thickness and conductivity), an accommodation coefficient must be provided for the estimation of the thermal resistance at the interface (Eq. 10). Furthermore, the model by Abu-Orabi distinguishes the droplet population in two categories, "small" droplets and "large" droplets, which are separated using the effective radius r_e, thus N_s (Eq. (15)). The model by Kim et *al.*, with a further step, adds the contact angle (otherwise assumed equal to 90° in the other correlations). In Table 1, all the input of the models are summarized and the values used for the comparison with experimental data measured by the present research group are reported.

Table 1. List of input variables considered in the models.

Variable	Value	Le Fevre & Rose	Abu-Orabi	Kim *et al.*
t_{SAT} [°C]	108	X	X	X
ΔT [°C]	5	X	X	X
δ [μm]	0.2		X	X
λ_{COAT} [W m^{-1} K^{-1}]	0.2		X	X
α [-]	1		X	X
N_S [m^{-2}]	10^{12}		X	X
θ [°]	90			X
θ_a [°]	88.6			X
θ_r [°]	63.4			X

In Fig. 1, a comparison between the droplets population calculated using all the three models is plotted. The droplet population is the number of drops (#) per unit area [m^{-2}] per unit radius [m^{-1}], thus it is expressed in [# m^{-3}]. The major difference among the models is, indeed, the introduction of the "small" droplet population for droplet radius ranging between r_{min} and r_e. In this zone, the population balance proposed by Le Fevre and Rose overestimates the number of "small" drops as compared to the other models, reaching a maximum of about 4 orders of magnitude near the r_{min} region. Assuming $\theta = 90°$, the model by Abu-Orabi and the model by Kim *et al.* predict the same frequency distribution. The small deviation in the "large" drop area is due to the different value of the maximum drop radius: in the case of Abu-Orabi model, a semi-empirical expression (Eq. (6)) is used, while the model by Kim *et al.* considers a force balance (in Eq. (25)).

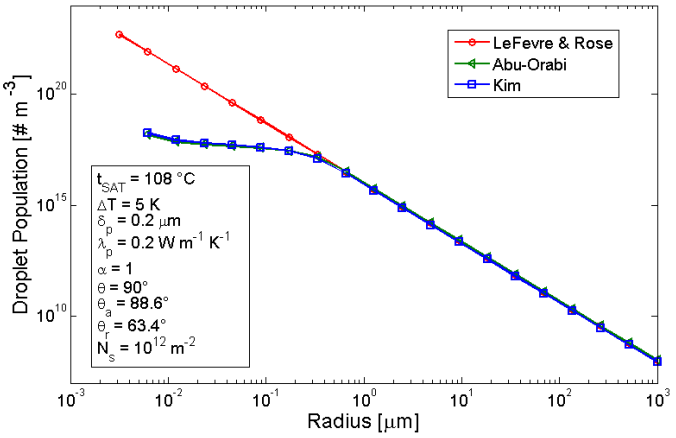

Fig. 1. Droplet population versus droplet radius calculated by Le Fevre & Rose, Abu-Orabi and Kim models.

In Fig. 2, the computed heat flow rate exchanged through a single droplet is plotted versus the droplet radius: the heat flow rate increases when the droplet becomes bigger. It should be noticed that, even adopting the same approach and imposing a contact angle equal to 90°, there is still a significant difference between the models by Abu-Orabi and Kim *et al.* In the model by Abu-Orabi, the conduction resistance is calculated considering a flat layer with thickness equal to the radius of the single drop (Eq. 8). Instead, Kim *et al.* accounts for the spherical shape of droplets (Eq. 22).

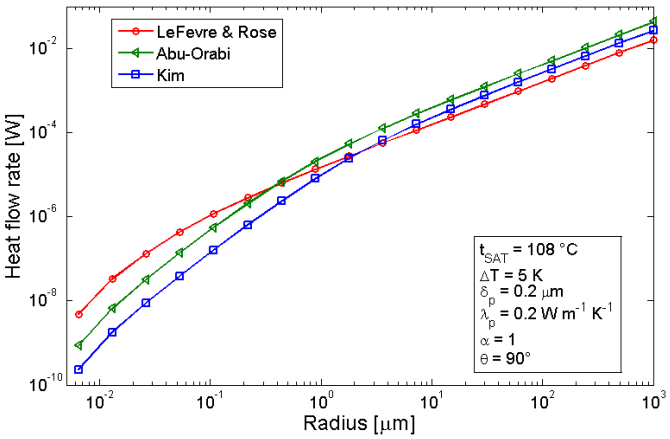

Fig. 2. Heat flow rate in a single drop versus the droplet radius calculated with the three models.

Considering a contact angle equal to 90°, the heat transfer resistance due to heat conduction in the droplet obtained from Eq. (22) (Kim *et al.* model) is about 50% higher compared to the value calculated with the model by Abu-Orabi (Eq. 8). This discrepancy results in lower heat flow rate computed with the Kim *et al.* model. The Le Fevre and Rose model considers the spherical shape of the droplet adding a constant corrective term (K_1), lower than 1, to account for the spherical shape of the drop.

COMPARISON WITH EXPERIMENTAL MEASUREMENTS

Experimental measurements have been performed by the present research group on aluminum samples, which were treated with a hydrophobic layer. The detailed procedure and the characterization of the sample is reported in [10].

The test rig is a thermosiphon loop and saturated vapor is used as operative fluid. The system consists of four main components (boiling chamber, test section, cooling water loop and post-condenser) and it allows simultaneous visualization of the condensation process. The sample is equipped with six thermocouples (two at the inlet, two in the middle and two at the outlet along the steam direction). The specimen is placed inside the test section: the treated surface is exposed to the vapor flow whereas the opposite surface is cooled by water. A detailed description of the experimental apparatus, the data reduction technique and the uncertainty analysis can be found in [11,12]. Fig. 3 reports an image taken during a dropwise condensation test on the aluminum sample: the area of analysis is highlighted.

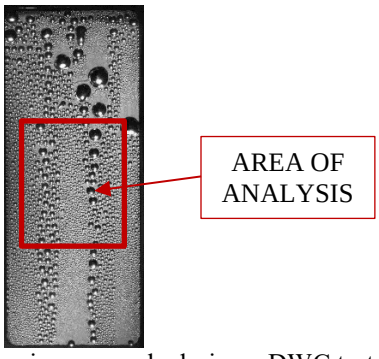

Fig. 3. Image of an aluminum sample during a DWC test.

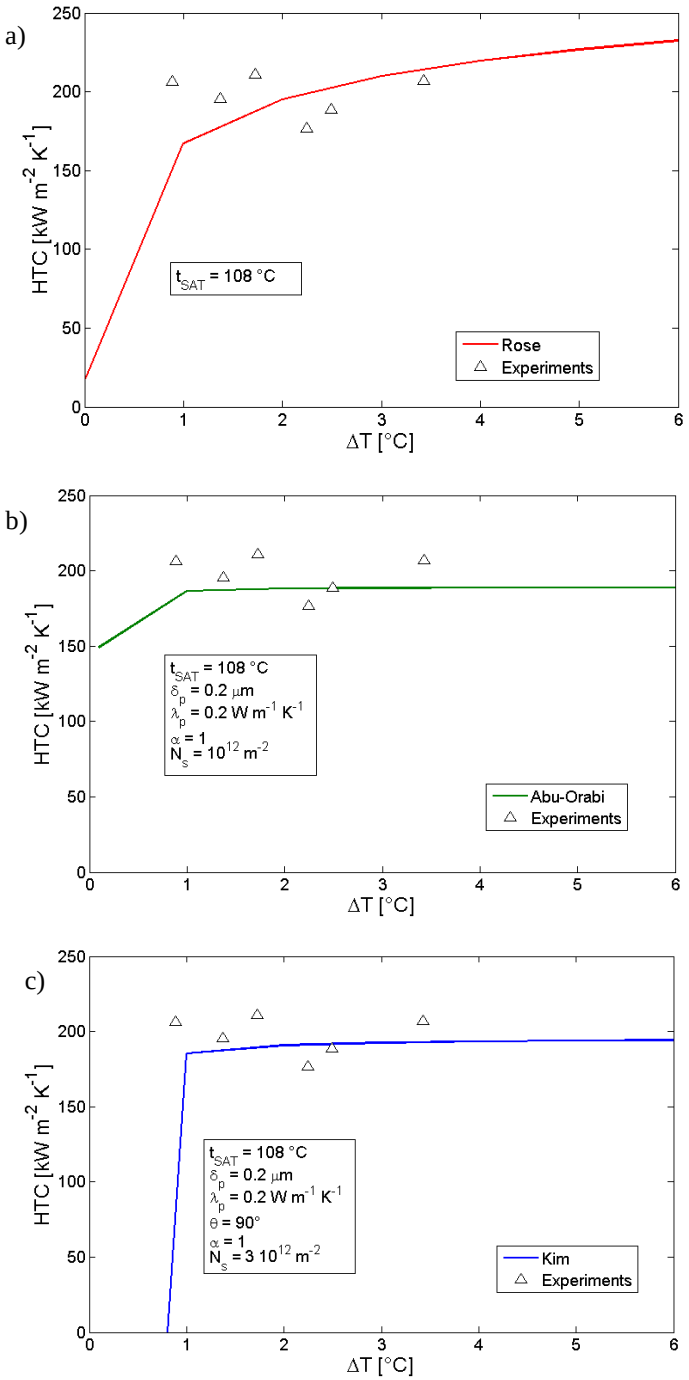

Fig. 4. Comparison between experimental and calculated heat transfer coefficients: a) Le Fevre and Rose model; b) Abu-Orabi model; c) Kim *et al.* model.

The main equations used for the determination of the heat transfer coefficient are summarized below. The local heat flux is obtained by applying the Fourier Law:

$$q_{loc} = \lambda_{al} \frac{\Delta T}{\Delta z} \tag{26}$$

The surface temperature T_{wall} is obtained from a linear interpolation of the temperatures measured by the thermocouples located at two different positions z_1 and z_2 form the surface of the sample:

$$T_{wall} = T_{z1} + (T_{z1} - T_{z2}) \frac{z_1}{z_2 - z_1} \tag{27}$$

For each operating condition, the measurements obtained at the area of analysis (Fig. 3) are reported. The main operative parameters during the tests are: t_{SAT} = 108°C, v_{VAP} = 2.6 m s^{-1}, coolant water temperature from 10°C to 85°C.

A comparison between the experimental data and the heat transfer coefficients predicted by the models is reported in Fig. 4. As shown in Table 1, each model needs different input and the values actually used to run the models are reported in each graph. The experimental campaign was performed with vapor flow and thus the vapor velocity can affect the droplet departure radius. In fact, in Eqs. (6) and (25) the vapor shear stress is not taken into account. For this reason, the maximum droplet radius is firstly measured from videos and then it is imposed to all the models as a boundary condition.

All the models display a good agreement with the experimental data, leading to a mean deviation of about 10%. It is worth mentioning that the Le Fevre and Rose model needs only the saturation temperature (and fluid properties) as input variables. In the case of Abu-Orabi and Kim *et al.* models, the number of nucleation sites is an input variable which is chosen here to get a good prediction of the data. The number of nucleation sites used in the Abu-Orabi model is different from the one adopted for the Kim *et al.* model: N_s used in the model by Kim *et al.* must be higher because the Kim *et al.* model predicts a lower droplet heat flow rate (Fig. 2).

IMAGES ANALYSIS

As mentioned before, the test section allows the direct visualization of the dropwise condensation (Fig. 3). From the analysis of the images, several fundamental aspects of the models can be verified. Table 2 shows the maximum radius r_{max} obtained from the models and from the visualizations. The measurements have been repeated several times in order to minimize the uncertainty.

Table 2. Comparison between experimental and theoretical droplet departing radius.

Model	Max. Radius [mm]
Le Fevre & Rose [2]	1.00
Kim *et al.* [4]	1.26
Experimental	0.93

The radius measured from the images is lower than the radius predicted by the two models (Eqs. (6) and (25)). A possible explanation is that such discrepancy is due to the speed of the vapor. In fact, an assumption of the models is that the steam is in a steady quiescent state, thus at zero velocity. The maximum droplet radius is important for the "large" droplet population (Eq. 5) and for the calculation of the heat flux being the upper limit of the integral in Eq. (1).

Another interesting information achievable by the videos is the "large" droplet population. Due to the resolution of the

optical system, only a small part of the population is appreciable, with a lower limit of about 0.1 mm. The measurement has been performed in the highlighted area of the sample (Fig. 3) and, in order to compare the data with Eq. (5), a statistical approach has been adopted. The experimental data have been divided in 20 classes and the number of drops for each class has been calculated. In order to make the comparison with the model, the integral of the distribution of the droplets for each previously defined class is computed. The number of droplets for each class is:

$$n^{\circ}\ drops\ per\ class = A \cdot \int_{r_a}^{r_b} N(r)dr \qquad (28)$$

where A is the area of the area of analysis, r_a and r_b are the minimum and maximum radius for the *i-th* class, respectively. Fig. 5 shows the result of the present analysis.

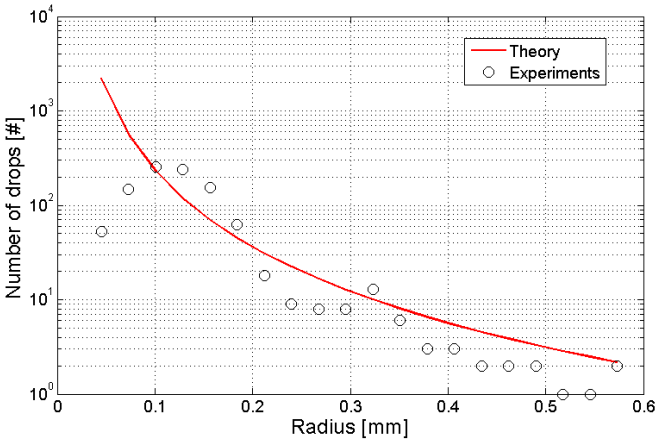

Fig. 5. Number of drops: calculated versus experimental results.

Even if the portion of measurable droplets size is very limited as compared to the enormous variety of droplets size (see Fig. 2), the measurements confirm Eq. (5). It can be noted that, since the droplets reach the maximum radius in the inlet zone and then they fall down, in the studied zone the maximum radius is significantly lower.

CONCLUSIONS

Three dropwise condensation models available in the literature and developed respectively by Le Fevre and Rose [2], Abu-Orabi [3] and Kim *et al.* [4] have been analyzed, highlighting analogies and differences between them. The models adopted a similar approach: the heat flux is calculated from the droplets population and from the heat flow rate through a single drop. The heat transfer coefficients calculated using these models are compared against experimental data taken by the present research group. Tests were performed during steam condensation over hydrophobic aluminum surfaces. The calculated heat transfer coefficients are in good agreement with measurements. Furthermore, high speed visualizations together with images analysis are employed to determine the population of droplets, at last for those that can be regarded as “large” droplets.

REFERENCES

[1] Schmidt, E., Schurig, W., Sellschopp, W., Versuche über die kondensation von wasserdampf in film- und tropfenform., Forsch. Im Ingenieurwes. 1 (1930) 53–63.

[2] J.W. Rose, Dropwise condensation theory and experiment: a review, Proc. Inst. Mech. Eng. Part A J. Power Energy. 216 (2002) 115–128. doi:10.1243/09576500260049034.

[3] M. Abu-Orabi, Modeling of heat transfer in dropwise condensation, Int. J. Heat Mass Transf. 41 (1998) 81–87. doi:10.1016/S0017-9310(97)00094-X.

[4] S. Kim, K.J. Kim, Dropwise Condensation Modeling Suitable for Superhydrophobic Surfaces, J. Heat Transfer. 133 (2011) 81502. doi:10.1115/1.4003742.

[5] N. Miljkovic, R. Enright, E.N. Wang, Modeling and Optimization of Superhydrophobic Condensation, J. Heat Transfer. 135 (2013) 111004. doi:10.1115/1.4024597.

[6] R. Enright, N. Miljkovic, J.L. Alvarado, K. Kim, J.W. Rose, Dropwise Condensation on Micro- and Nanostructured Surfaces, Nanoscale Microscale Thermophys. Eng. 18 (2014) 223–250. doi:10.1080/15567265.2013.862889.

[7] S. Khandekar, K. Muralidhar, Dropwise Condensation on Inclined Textured Surfaces, Springer, 2014.

[8] H. Tanaka, A Theoretical Study of Dropwise Condensation, J. Heat Transfer. 97 (1975) 72–78. http://dx.doi.org/10.1115/1.3450291.

[9] H.W. Wen, R.M. Jer, On the heat transfer in dropwise condensation, Chem. Eng. J. 12 (1976) 225–231. doi:10.1016/0300-9467(76)87016-5.

[10] P. Innocenzi, M.O. Abdirashid, M. Guglielmi, Structure and Properties of Sol-Gel Coatings from Methyltriethoxysilane and Tetraethoxysilane, J. Sol-Gel Sci. Technol. 3 (1994) 47–55. doi:10.1007/BF00490148.

[11] D. Del Col, R. Parin, A. Bisetto, S. Bortolin, A. Martucci, Film condensation of steam flowing on a hydrophobic surface, Int. J. Heat Mass Transf. 107 (2017) 307–318. doi:10.1016/j.ijheatmasstransfer.2016.10.092.

[12] A. Bisetto, S. Bortolin, D. Del Col, Experimental analysis of steam condensation over conventional and superhydrophilic vertical surfaces, Exp. Therm. Fluid Sci. 68 (2015) 216–227. doi:10.1016/j.expthermflusci.2015.04.019.